

A Novel Dipolar Dephasing Method for the Slow Magic Angle Turning Experiment

Jian Zhi Hu,¹ Craig M. V. Taylor,* Ronald J. Pugmire,† and David M. Grant

†Departments of Chemistry and Chemical and Fuels Engineering, University of Utah, Salt Lake City, Utah 84112;
and *Los Alamos National Laboratory, Los Alamos, New Mexico 87545

Received October 25, 2000; revised May 16, 2001; published online August 1, 2001

Complete suppression of the resonances from protonated carbons in a slow magic angle spinning experiment can be achieved using five dipolar dephasing (Five-DD) periods distributed in one rotor period. This produces a spectrum containing only the spinning sidebands (SSB) from the nonprotonated carbons. It is shown that the SSB patterns corresponding to the nonprotonated carbons are not distorted over a wide range of dipolar dephasing times. Hence, this method can be used to obtain reliable principal values of the chemical shift tensors for each nonprotonated carbon. The Five-DD method can be readily incorporated into isotropic–anisotropic 2D experiments such as FIREMAT and 2D-PASS to facilitate the measurement of the ¹³C chemical shift tensors in complex systems. © 2001 Academic Press

Key Words: dipolar dephasing in slow MAT experiments; chemical shift tensor; FIREMAT and 2D-PASS.

1. INTRODUCTION

Since its implementation two decades ago (1, 2), the dipolar dephasing experiment remains one of the most useful methods for simplifying a ¹³C CP/MAS spectrum obtained from a rigid solid. By introducing an interrupted decoupling period of about 40 μs following the conventional cross-polarization (2, 3) in the proton channel, a ¹³C spectrum of nonprotonated and methyl carbons is obtained while suppressing the resonances from both the CH and CH₂ carbons. The coupled protons in CH and CH₂ groups suppress the resonance signals of the corresponding ¹³C nuclei. Subsequent modifications (4, 5) have been made by including an echo sequence consisting of a π-pulse in the ¹³C or both ¹H and ¹³C channels to eliminate the first-order phase distortions in spectra associated with the initial dipolar dephasing method. Rotor synchronization has also been proposed (6) to suppress the dephasing effect due to the chemical shift anisotropy contribution. Dipolar dephasing methods have been proposed to obtain the relative ratio of protonated and nonprotonated carbons in the aromatic part of complex substances such as fossil fuels including coals (5). This method has been especially attractive for separating severely overlapped

resonances corresponding to protonated and nonprotonated carbons.

In high-resolution ¹³C CP/MAS experiments, a sample-spinning rate larger than the width of the chemical shift tensor produces an isotropic shift spectrum of a powder sample. Unfortunately, the chemical shift tensor information (e.g., the three principal values of the tensor) is lost at high spinning rates. When a sample-spinning rate less than the tensor width is used, the powder pattern corresponding to the shift tensor is exhibited as sideband patterns separated by the spinning frequency. The principal values of the shift tensor can be obtained from the sideband patterns using the Herzfeld and Berger method (7). Experimental techniques that simplify the complexity of overlapping *slow MAS* spectra, referred to as MAT (magic angle turning) spectra, become especially important when studying a system with complex molecular structure.

This paper describes a method employing the dipolar dephasing experiment in MAT experiments wherein powder pattern distortion is essentially eliminated, e.g., a MAT spectrum containing only nonprotonated and methyl carbons with spinning sideband patterns undistorted relative to those observed when no dipolar dephasing is applied. Hence, the principal values of the shift tensors for the nonprotonated carbons can be extracted with a high degree of accuracy from the dipolar dephased MAT experiment. The key to the success of this experiment lies in properly inserting five dipolar dephasing (Five-DD) periods (that are evenly, or approximately evenly, spaced around one rotor period) into the 5–π pulse variant of the MAT class of experiments. The Five-DD method can be incorporated into two types of 2D MAT isotropic–anisotropic correlation experiments, i.e., the FIREMAT experiment (8) developed in this laboratory and the 2D-PASS experiment reported by Levitt and co-workers (9).

2. EXPERIMENTAL

The pulse sequences used for the dipolar dephasing experiment are illustrated in Fig. 1. Figure 1a is one of the versions used by Newman (6), in which the π pulse is synchronized to multiple rotor periods. The resultant spectrum using this echo sequence is well phased. The Five-DD pulse sequence in Fig. 1b

¹ Current address: Pacific Northwest National Laboratory, P.O. Box 999, MS K8-98, Richland, WA 99352.

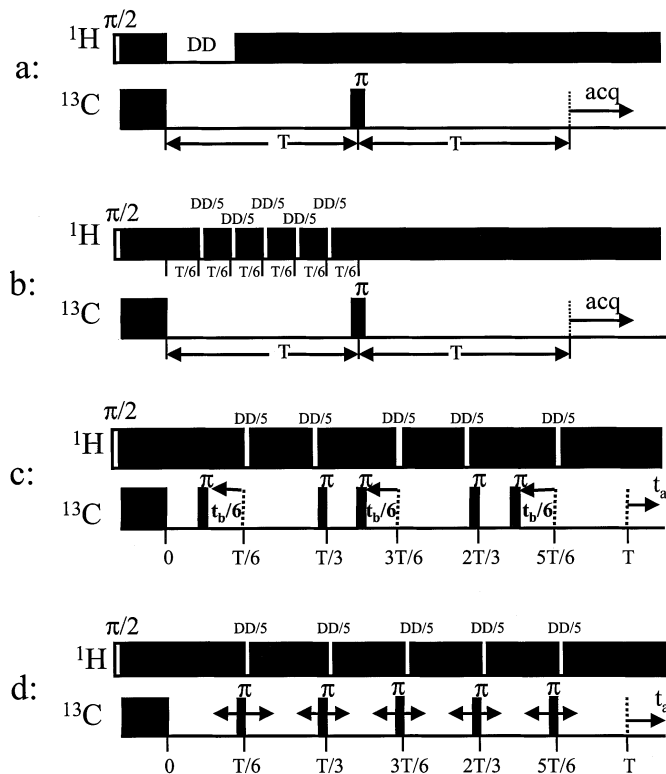


FIG. 1. (a) The traditional dipolar dephasing pulse sequence with one dephasing period. (b) The dipolar dephasing pulse sequence with the dephasing time divided into five subsegments evenly distributed around one rotor period, i.e., the Five-DD sequence. (c) FIREMAT + Five-DD. (d) 2D-PASS + Five-DD, where the positions of π -pulses shown are corresponding to the first evolution increment of the 2D experiment; the π -pulses can move in both directions indicated by the arrows with timings of the subsequent evolution increments for each individual π -pulse specified in Ref. (9). The same pulse phase cycling as those in the FIREMAT experiment (Ref. (8)) was employed in the 2D-PASS experiment in this study. “T” denotes the rotor period in all the pulse sequences. A value of DD/5 larger than about $14 \mu\text{s}$ is required to completely suppress the CH and CH_2 signals.

is an extension of Fig. 1a, where the dipolar dephasing time (DD) is divided into five equal segments evenly distributed at one rotor period. Figure 1c is the modified version of the FIREMAT pulse sequence in which the Five-DD sequence is incorporated. Since the zero evolution time variable $t_b/6$ starts at $T/6$, $3T/6$, and $5T/6$, and ends one acquisition dwell time away from 0, $T/3$, and $2T/3$, it is impossible to distribute the five dephasing periods evenly around one rotor period. Instead, the second and the fourth dephasing periods are placed immediately before the $T/3$ and $2T/3$ π -pulses, respectively, in the periodic rotation of the sample. Figure 1d exhibits the 2D-PASS sequence in which the Five-DD pulse sequence has been incorporated. In the 2D-PASS experiment every π -pulse is initiated according to the times specified in the PASS timing table (9) given originally and the five dephasing periods are placed immediately following each π -pulse. In these experiments, the dephasing periods constitute a small time fraction of the rotor period and adverse

impact of these anomalous placements of dephasing periods has not been observed.

All the experiments were performed on a Chemagnetics CMX-200 NMR spectrometer operating at a field of 4.7 T. The corresponding Larmor frequencies for ^{13}C and ^1H are 50.305 and 200.045 MHz, respectively. A standard CP/MAS probe with a 7.5-mm rotor and a Chemagnetics MAS speed controller were used. Multiple marks were placed evenly around the sample rotor. In this way, a spinning accuracy of about ± 0.1 to 1 Hz was achieved by using only the Chemagnetics MAS speed controller. The RF field strength for both ^{13}C and ^1H channels is about 62.5 kHz, corresponding to a $\pi/2$ pulse width of $4 \mu\text{s}$.

3. RESULTS AND DISCUSSIONS

Figure 2 presents eight ^{13}C CP/MAS spectra with variable dipolar dephasing times (DD) obtained from a powdered sample of glycine using the pulse sequence in Fig. 1 at a sample-spinning rate of 300 ± 1 Hz. With dephasing times up to $100 \mu\text{s}$, one is unable to completely suppress the signal from the CH_2 carbon. In addition, considerable distortion of the spinning side-band pattern for the nonprotonated carbon is observed when dipolar dephasing times larger than $60 \mu\text{s}$ are used. The pulse

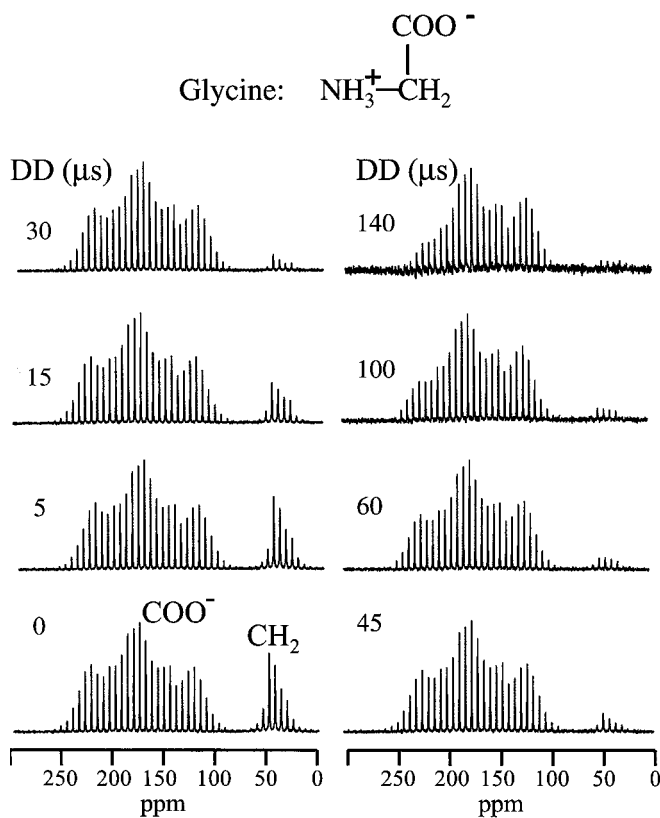


FIG. 2. The ^{13}C CP/MAS spectra of 99% ^{15}N -labeled glycine acquired using the pulse sequence in Fig. 1a employing variable dipolar dephasing times (DD) and a sample-spinning rate of 300 Hz.

sequence in Fig. 1a is essentially a separated-local-field pulse sequence reported previously by Roberts *et al.* (10), omitting homonuclear dipolar decoupling among protons. The amplitude and the phase of the acquired FID for different crystallites in the powder sample are correlated with the $^{13}\text{C}-^1\text{H}$ dipolar coupling during the dephasing time. The dephasing effect on the spectrum may be explained qualitatively such that the crystallites experiencing larger dipolar coupling decay faster than those possessing smaller dipolar coupling. Since the sample rotates at the magic angle and at a relatively slow spinning rate, the dephasing time accounts for only a small fraction of the rotor period. Crystallites whose $^{13}\text{C}-^1\text{H}$ dipolar vectors orient initially along or near the magic angle will remain near the magic angle during the dephasing time and hence experience a weaker dipolar coupling during the entire dipolar dephasing time. In the case of CH_2 groups, two heteronuclear dipolar couplings are present and, for a large number of configurations, these interactions nearly cancel each other. Sometimes these couplings cancel because one proton spin is up and the other is down; or they cancel because the geometric factors have opposite sign, resulting in a large intensity at zero frequency in the dipolar spectrum of carbons in a CH_2 group (11). As a result, the magnetization persists for an extended dephasing time. The corresponding spinning sideband (SSB) powder patterns of nonprotonated carbons can be distorted when the spins experience a variety of remote $^{13}\text{C}-^1\text{H}$ dipolar couplings due to different orientations relative to the external magnetic field direction. For instance, the remote $^1\text{H}-^{13}\text{C}$ dipolar coupling for the nonprotonated carbon in glycine oriented nearly along the δ_{11} component is apparently larger than those associated with the δ_{22} and δ_{33} components.

By dividing the dipolar dephasing time into five segments distributed around one rotor period, each crystallite will begin its evolution with a different orientation, and hence experience a different $^{13}\text{C}-^1\text{H}$ dipolar coupling during each dipolar dephasing period. The result is an averaged dephasing effect. Figure 3 presents the spectra acquired with and without dipolar dephasing applied using the Five-DD pulse sequence in Fig. 1b at spinning rates from 150 to 800 Hz. It is clear that complete suppression of the CH_2 resonance is achieved by dividing the total dephasing time of $100\ \mu\text{s}$ into five segments distributed evenly around one rotor period. The SSB powder patterns for the nonprotonated carbon with and without dipolar dephasing applied are essentially the same at all the spinning rates investigated. The relative sensitivity for the nonprotonated carbon with and without application of the dipolar dephasing sequence will be addressed later (see Fig. 10).

The FIREMAT spectra of a powder sample of glycine, with and without the Five-DD pulse sequence incorporated, are illustrated in Fig. 4. In the standard FIREMAT spectra of glycine (left side in Fig. 4), the SSB powder patterns for the CH_2 and the nonprotonated carbon are isolated according to their isotropic chemical shift values. In the FIREMAT + Five-DD spectra (right side in Fig. 4), the CH_2 SSB pattern is completely removed using a total dipolar dephasing time of $100\ \mu\text{s}$. Little distortion

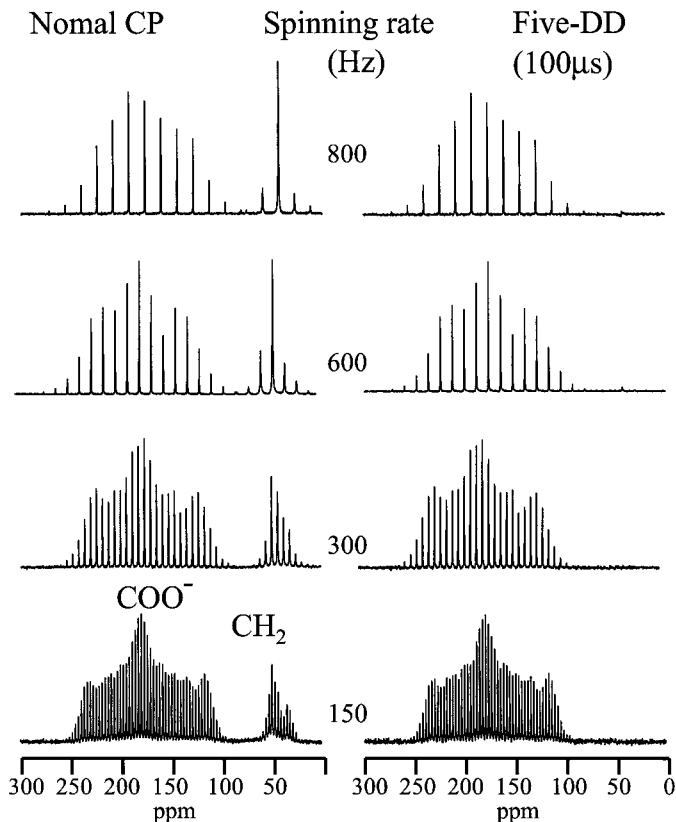


FIG. 3. The ^{13}C CP/MAS spectra of 99% ^{15}N -labeled glycine acquired using the pulse sequence in Fig. 1b with (right) and without (left) employing a total dipolar dephasing time of $100\ \mu\text{s}$ and at sample-spinning rates ranging from 150 to 800 Hz.

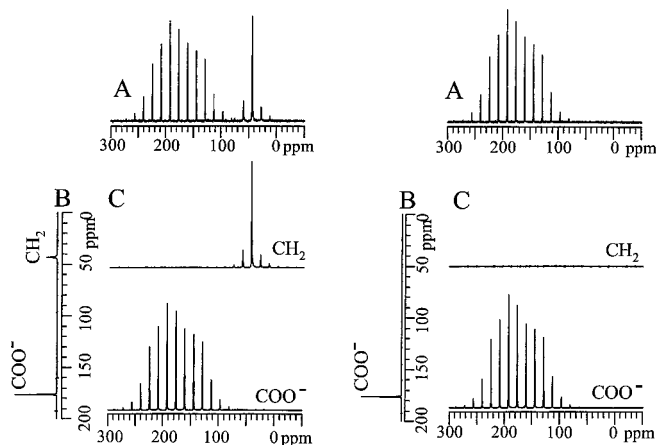


FIG. 4. (Left) The standard ^{13}C FIREMAT spectra of 99% ^{15}N -labeled glycine. (Right) The ^{13}C FIREMAT + Five-DD spectra of glycine with a total dipolar dephasing time of $100\ \mu\text{s}$. The spectra shown sequentially are projection along the acquisition dimension (A), projection along the isotropic dimension (B), and FIREMAT isolated spinning sideband for each carbon (C). These spectra were acquired using 16 evolution increments and a cross-polarization contact time of 4 ms at a sample-spinning rate of 800 Hz. For each evolution increment, 288 scans with a recycle delay time of 3 s were acquired (left) and 960 scans with a recycle delay time of 3 s were acquired (right).

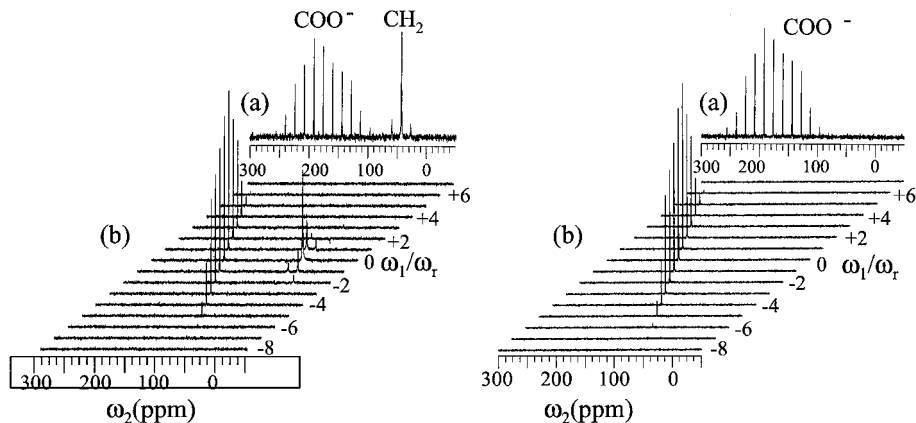


FIG. 5. (Left) The stacked plot of standard ^{13}C 2D-PASS spectra of 99% ^{15}N -labeled glycine acquired at a sample-spinning rate of 800 Hz. Sixteen pulse sequences (i.e., 16 evolution increments) were used in the 2D-PASS experiment with a contact time of 4 ms, 16 scans with a recycle delay time of 4 s for each pulse sequence. (a) The projection along the acquisition dimension and (b) the 2D-PASS spectrum showing sidebands separated in the ω_1 dimension. The ω_1 slices are labeled with the order of the sidebands. (Right) The stacked plot of the dipolar dephased ^{13}C 2D-PASS spectra of 99% ^{15}N -labeled glycine acquired using the pulse sequence in Fig. 1d with a total dephasing time of 100 μs . The other experimental parameters were the same as those on the left except 96 scans were accumulated for each pulse sequence.

is evident in the sideband pattern of the nonprotonated carbon when FIREMAT is combined with the Five-DD method.

The 2D-PASS spectra on a powder sample of glycine with and without the particular modifications of the Five-DD pulse sequence are illustrated in Fig. 5. In the standard 2D-PASS spectrum, the sidebands corresponding to the nonprotonated carbon are separated by the order of side bands. *Some residual dipolar coupling pattern, manifested by additional sidebands, is observed for the CH_2 carbon (the left side spectra in Fig. 5).* In the 2D-PASS + Five-DD all the resonances corresponding to the CH_2 carbon are completely removed, leaving only the 2D-PASS pattern of the nonprotonated carbon. The SSB powder patterns with and without Five-DD for the nonprotonated carbon are essentially the same, a result similar to that obtained from FIREMAT + Five-DD. The principal values of ^{13}C CSA for the nonprotonated carbon in glycine obtained from the various spectra are essentially the same within the experimental error and the results are summarized in Table 1.

Removal of the SSB from the protonated carbons facilitates the measurement of the ^{13}C CSA principal values in a system with complex molecular structure. Examples are provided in Figs. 6–8 for 1-decylpyrene. The conventional high-speed

(4-kHz) ^{13}C CP/MAS with (top) and without (bottom) dipolar dephasing are given in Fig. 6. The resonances corresponding to carbon sites 10a, 10b, and 10c are typically overlapped with those of protonated aromatic carbons, and these three shift tensors would be difficult to obtain if standard FIREMAT or 2D-PASS experiments were used. The measurement is simplified by using FIREMAT + Five-DD or 2D-PASS + Five-DD as summarized respectively in Figs. 7 and 8. Herein, only the SSB

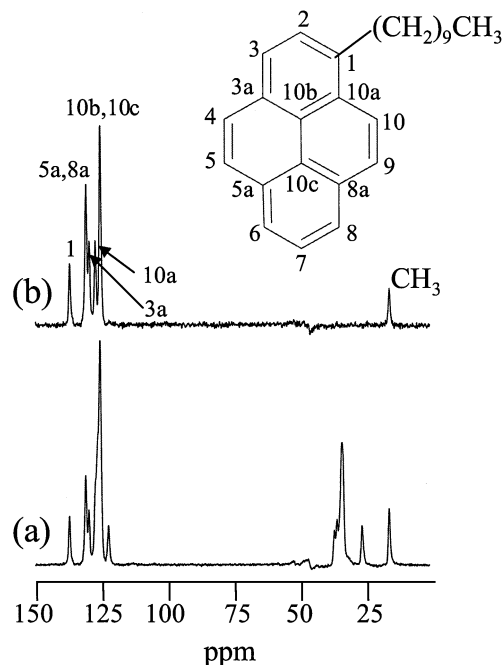


FIG. 6. The ^{13}C CP/MAS spectra of 1-decylpyrene acquired at a sample-spinning rate of 4 kHz. (a) The traditional CP/MAS spectrum. (b) The traditional dipolar dephased spectrum with a dephasing time of 45 μs .

TABLE 1

The Experimental Principal Values of ^{13}C CSA of the Nonprotonated Carbon in Glycine Obtained from the Various Methods

Method	δ_{11} (ppm)	δ_{22} (ppm)	δ_{33} (ppm)	δ_{iso} (ppm)
FIREMAT	245	181	104	176.5
FIREMAT + Five-DD ^a	245	181	103	176.5
2D-PASS	243	181	105	176.5
2D-PASS + Five-DD ^a	244	181	105	176.5

^a The total dipolar dephasing time is 100 μs .

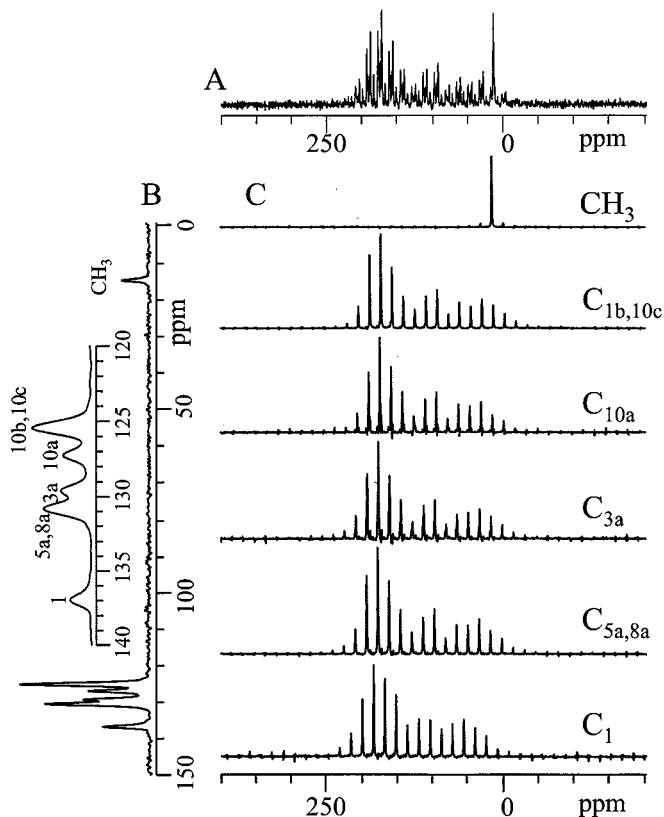


FIG. 7. ^{13}C FIREMAT + Five-DD spectra of 1-decylpyrene acquired using the pulse sequence in Fig. 1c with a total dephasing time of $100\ \mu\text{s}$, a contact time of 4 ms, and at a sample-spinning rate of 800 Hz. Sixteen evolution increments were acquired with 384 scans and a recycle delay time of 10 s for each increment. A, B, and C are projection along the acquisition dimension, projection along the isotropic dimension, and FIREMAT isolated spinning sideband powder pattern for each carbon, respectively.

powder patterns corresponding to the nonprotonated carbons and the methyl carbon remain.

In Fig. 7 the methyl carbon exhibits an intense center band at a spinning rate of 800 Hz due to the small span of its chemical shift tensor. There are five nonprotonated resonances observed in the aromatic spectral region (isotropic shift >90 ppm). Note

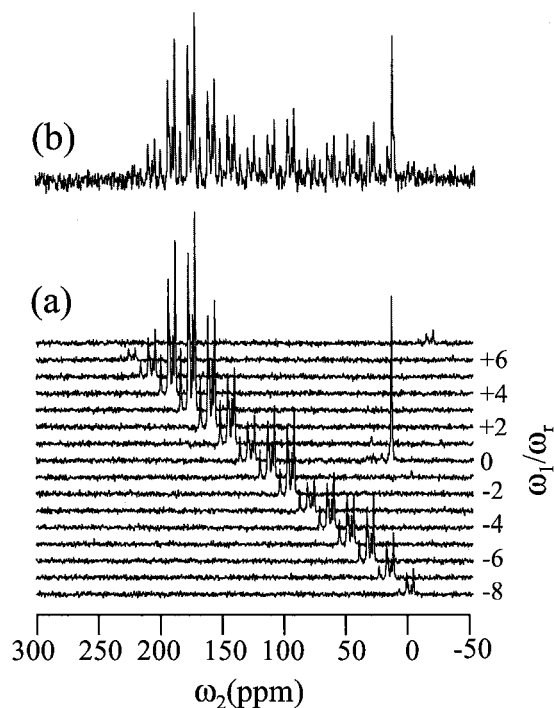


FIG. 8. (a) The stacked plot of ^{13}C 2D-PASS + Five-DD spectra of 1-decylpyrene acquired using the pulse sequence in Fig. 1d with a total dephasing time of $100\ \mu\text{s}$, a contact time of 4 ms, and at a sample-spinning rate of 800 Hz. Sixteen evolution increments were acquired with 384 scans and a recycle delay time of 10 s for each pulse sequence. (b) Projection along the acquisition dimension.

in the inset that both sets of resonances for 5a and 8a and also for 10b and 10c exhibit degeneracy in the isotropic shifts. The principal values of the ^{13}C CSA were obtained by fitting the FID for each isolated SSB family using the band-matrix method (12) and the results are summarized in Table 2.

The 2D-PASS + Five-DD results are given in Fig. 8 for the nonprotonated carbons and the methyl carbon with the SSB intensities corresponding to each SSB order for each spectral slice readily separable in Fig. 8. The principal values of the ^{13}C CSA were obtained by fitting the signal intensity using the Herzfeld

TABLE 2

The Experimental ^{13}C Principal Values in 1-Decylpyrene Obtained from the 2D-PASS + Five-DD and the FIREMAT + Five-DD: The Results from Triple-Echo MAT Are also Included for Comparison

Isotropic shift δ_{iso}	Triple-echo MAT ^a			FIREMAT + Five-DD			2D-PASS + Five-DD			Assignments ^b
	δ_{11}	δ_{22}	δ_{33}	δ_{11}	δ_{22}	δ_{33}	δ_{11}	δ_{22}	δ_{33}	
125.5	199	192	-16	201	190	-15	205	186	-15	$\text{C}_{10\text{b},10\text{c}}$
127.4	204	183	-4	204	181	-2	206	180	-4	$\text{C}_{10\text{a}}$
129.7	—	—	—	210	185	-6	210	185	-6	$\text{C}_{3\text{a}}$
130.9	212	188	-8	212	188	-7	213	186	-7	$\text{C}_{5\text{a},8\text{a}}$
137.1	222	177	13	222	178	11	222	177	11	C_1

^a The data were obtained at a sample-spinning rate of 30 ± 0.2 Hz. (—) Data are not available due to insufficient resolution along the isotropic dimension.

^b The assignments of the resonances were obtained from an extensive study of the shift tensor in 1-decylpyrene using triple-echo MAT (13), FIREMAT, and quantum chemistry theoretical predictions of the shift tensor, which will be correlated and discussed in a separate paper.

and Berger method (7) and the results are summarized in Table 2.

It is obvious that data obtained from both FIREMAT + Five-DD and 2D-PASS + Five-DD are in agreement within the experimental error range. These data also agree with those obtained from the triple-echo MAT (13) experiment that used a much slower sample-spinning rate (i.e., 30 Hz).

Because the 2D-PASS experiment separates SSBs by order, the principal values of ^{13}C species can be measured in a complex

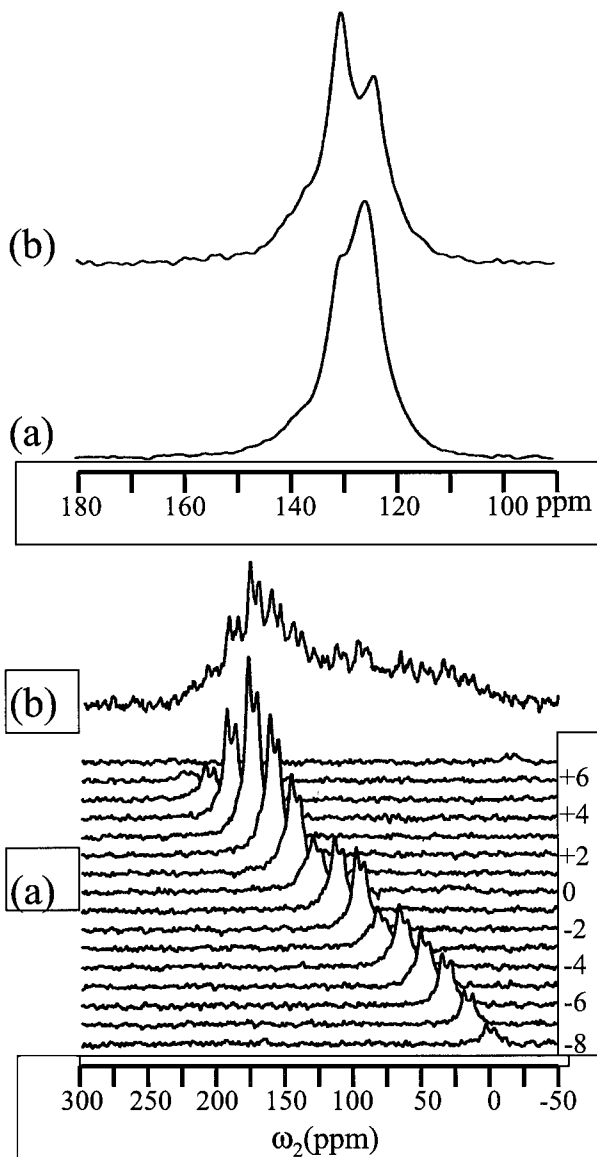


FIG. 9. (Top) The ^{13}C CP/MAS spectra of pyrene-soot (1410 K) acquired at a sample-spinning rate of 4 kHz. (a) The traditional CP/MAS spectrum. (b) The traditional dipolar dephased spectrum with a dephasing time of $45\ \mu\text{s}$. (Bottom) (a) The stacked plot of ^{13}C 2D-PASS + Five-DD spectra of pyrene-soot (1410 K) acquired using the pulse sequence in Fig. 1c with a total dephasing time of $100\ \mu\text{s}$, a contact time of 4 ms, and at a sample-spinning rate of 800 Hz. Sixteen pulse sequences were acquired with 12,000 scans and a recycle delay time of 1 s for each pulse sequence. (b) Projection along the acquisition dimension.

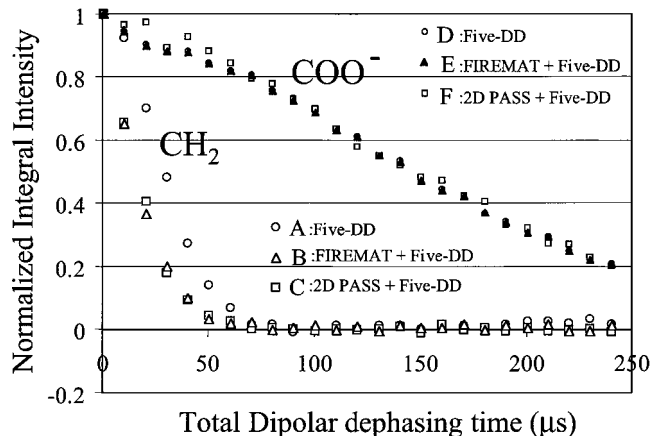


FIG. 10. The integral signal intensity of the CH_2 and the nonprotonated carbon (COO^-) in 99% ^{15}N -labeled glycine as a function of the total dephasing time using the pulse sequences in Figs. 1b (Five-DD), 1c (FIREMAT + Five-DD), and 1d (2D-PASS + Five-DD), respectively, and at a sample-spinning rate of $600 \pm 1\ \text{Hz}$. In both FIREMAT + Five-DD and 2D-PASS + Five-DD cases, the first evolution increment of the respective 2D experiment was used to simulated the dipolar dephasing effect with variable dephasing times.

system, where the isotropic chemical shifts are severely overlapped. An example is provided in Fig. 9 using an aerosol/soot sample that was prepared and collected at a temperature of 1410 K (14) using pyrene as the starting material. The 2D-PASS experiment appears to offer some benefits in the analysis of a heterogeneous cluster of resonance lines because the TIGER (15) component of FIREMAT suffers some modeling problems with highly overlapping heterogeneous resonance lines.

Figure 10 summarizes the signal intensity of both the CH_2 and the nonprotonated carbons in glycine versus the total dephasing time using the pulse sequences in Figs. 1b–1d, respectively. In general, complete suppression of the CH_2 signal can be achieved using a total combined dephasing time of about $70\ \mu\text{s}$. The overall dephasing behavior for FIREMAT + Five-DD and PASS + Five-DD are similar even though the timings for the dipolar dephasing segments are different. The CH_2 signal decays appreciably faster in both the FIREMAT + Five-DD and PASS + Five-DD cases relative to that obtained using the Five-DD sequence. The similarity of FIREMAT and 2D-PASS results should not be unusually surprising as both methods are based on the $5\text{-}\pi$ pulse phase-modulated experiment. We are engaged in a more complete comparative analysis of these two related methods.

4. CONCLUSIONS

A method has been developed to implement dipolar dephasing techniques that are especially useful for ^{13}C MAT experiments. By dividing the total dipolar dephasing period into multiple intervals around one rotor period, it is possible to suppress the SSB corresponding to the protonated carbons in a rigid solid while leaving a spectrum containing only the SSB for the

nonprotonated and methyl carbons. The signal from the methyl carbons persists due to fast rotation about the C_3 symmetric axis even though the SSB pattern is distorted somewhat under proton dephasing. It is shown that the distortion of the SSB patterns for the nonprotonated carbons is minimized by dividing the total dephasing time into five sub-dipolar dephasing times either evenly spaced in the simple 1D experiment, or relative to the π -pulses in the FIREMAT and 2D-PASS experiments. This procedure simplifies the measurement of the ^{13}C chemical shift tensors by removing the SSB patterns for the protonated carbons in multidimensional MAT experiments with little, if any, distortion of the powder pattern of the nonprotonated carbons. It is also shown that the Five-DD method can be readily incorporated into 2D isotropic–anisotropic correlation experiments, i.e., the FIREMAT and the 2D-PASS, to simplify the measurement of ^{13}C CSA in a system with complex molecular structures.

ACKNOWLEDGMENTS

This work was supported by the Office of Basic Energy Science of DOE under Grant DE FG02-94 ER 14452; by the National Institute of Health, General Medical Sciences, under GM 08521-37; and by the Pittsburgh Technology Center (PETC) by a contract to the Consortium for Fossil Fuel Liquefaction Science. Dr. Jian Zhi Hu was supported by a Fellowship from the Green Chemistry Program of Los Alamos National Laboratory through the Associated Western Universities. The authors are especially grateful to Dr. D. W. Alderman and M. S. Solum for their assistance with the data processing of the FIREMAT and 2D-PASS data.

REFERENCES

1. M. Alla and E. Lippmaa, *Chem. Phys. Lett.* **37**, 260 (1976).
2. S. J. Opella and M. H. Frey, *J. Am. Chem. Soc.* **101**, 5854 (1979).
3. P. DuBois Murphy, T. J. Cassady, and B. C. Gerstein, *Fuel* **61**, 1233 (1982).
4. L. B. Alemany, D. M. Grant, T. D. Alger, and R. J. Pugmire, *J. Am. Chem. Soc.* **105**, 6697 (1983).
5. M. S. Solum, R. J. Pugmire, and D. M. Grant, *Energy Fuels* **3**, 187 (1989).
6. R. H. Newman, *J. Magn. Reson.* **96**, 370 (1992).
7. J. Herzfeld and A. E. Berger, *J. Chem. Phys.* **73**, 6021 (1980).
8. D. W. Alderman, G. McGeorge, J. Z. Hu, R. J. Pugmire, and D. M. Grant, *Mol. Phys.* **95**, 1113 (1998).
9. O. N. Antzutkin, S. C. Shekar, and M. H. Levitt, *J. Magn. Reson. A* **115**, 7 (1995).
10. J. E. Roberts, G. S. Harbison, M. G. Munowitz, J. Hertfeld, and R. G. Griffin, *J. Am. Chem. Soc.* **109**, 4163 (1987).
11. K. Schmidt-Rohr and H. W. Spiess, "Multidimensional Solid-State NMR and Polymers," Academic Press, San Diego (1994).
12. N. K. Sethi, D. W. Alderman, and D. M. Grant, *Mol. Phys.* **71**, 217 (1990).
13. J. Z. Hu, A. M. Orendt, D. W. Alderman, R. J. Pugmire, C. Ye, and D. M. Grant, *Solid State NMR* **3**, 181 (1994).
14. M. S. Solum, A. F. Sarofim, R. J. Pugmire, T. H. Fletcher, and H. Zhang, *Energy Fuels*, in press (2001).
15. G. McGeorge, J. Z. Hu, C. L. Mayne, D. W. Alderman, R. J. Pugmire, and D. M. Grant, *J. Magn. Reson.* **129**, 134 (1997).